Physics Letters B 765 (2017) 99–103

Contents lists available at ScienceDirect

Physics Letters B

www.elsevier.com/locate/physletb

# Fusion enhancement at near and sub-barrier energies in $^{19}O + ^{12}C$

Varinderjit Singh [a], J. Vadas [a], T.K. Steinbach [a], B.B. Wiggins [a], S. Hudan [a], R.T. deSouza [a,*], Zidu Lin [b], C.J. Horowitz [b], L.T. Baby [c], S.A. Kuvin [c], Vandana Tripathi [c], I. Wiedenhöver [c], A.S. Umar [d]

[a] Department of Chemistry and Center for Exploration of Energy and Matter, Indiana University, 2401 Milo B. Sampson Lane, Bloomington, IN 47408, USA
[b] Department of Physics and Center for Exploration of Energy and Matter, Indiana University, 2401 Milo B. Sampson Lane, Bloomington, IN 47408, USA
[c] Department of Physics, Florida State University, Tallahassee, FL 32306, USA
[d] Department of Physics and Astronomy, Vanderbilt University, Nashville, TN 37235, USA

ARTICLE INFO

*Article history:*
Received 16 September 2016
Received in revised form 28 October 2016
Accepted 7 December 2016
Available online 12 December 2016
Editor: D.F. Geesaman

*Keywords:*
Near-barrier fusion
Neutron-rich fusion
RIB fusion
Fusion enhancement

ABSTRACT

Measuring the fusion excitation function for an isotopic chain of projectile nuclei provides a stringent test of a microscopic description of fusion. We report the first measurement of the fusion excitation function at near-barrier energies for the $^{19}O + ^{12}C$ system. The measured excitation function is compared with the fusion excitation function of $^{18}O + ^{12}C$. A significant enhancement in the fusion probability of $^{19}O$ ions with a $^{12}C$ target as compared to $^{18}O$ ions is observed. The experimental cross-sections observed at near-barrier energies are compared with a state-of-the-art microscopic model.



## 1. Introduction

While the fusion of both light and heavy $\beta$-stable nuclei has been studied for several decades, only recently has the investigation of fusion of neutron-rich nuclei become feasible due to radioactive beam facilities [1–5]. In particular, examination of the fusion excitation function for an isotopic chain of neutron-rich nuclei represents an unique opportunity. Since the charge distribution of the neutron-rich projectile nuclei is essentially unaffected by the additional neutrons, the repulsive Coulomb potential is largely unchanged. Consequently, the comparison of the fusion excitation functions for the different projectiles provides access to the change in the attractive nuclear potential with an increasing number of neutrons. As the initial step in fusion at near-barrier energies involves overlap of the low density tails of the nuclear matter distribution, these reactions provide a sensitive probe of the composition and extent of the nuclear surface. An accurate microscopic description of the fusion of neutron-rich nuclei is thus relevant to the asymmetry term in the nuclear equation-of-state and in particular its density dependence [6].

Despite the opportunity presented to learn about structure and dynamics of low-density nuclear matter by examining the fusion of light nuclei, relatively few isotopic chains have been investigated, as radioactive beams are necessary. An initial measurement of fusion induced with a neutron-rich oxygen nucleus, $^{20}O$, on a $^{12}C$ target suggested an enhancement of the fusion probability as compared to a standard fusion–evaporation model [7]. However, technical difficulties in the experiment prevented extraction of the total fusion cross-section. Recently, the fusion of $^{10,14,15}C + ^{12}C$ has been investigated using a novel active target approach [8]. At the above barrier energies studied, no significant fusion enhancement was observed relative to a simple barrier penetrability model. However, close examination of the $^{15}C + ^{12}C$ data presented reveals that at lowest energies measured, the data slightly exceed the model predictions. It can be argued on general grounds that fusion enhancement is best studied at near and below barrier energies. At low incident energies, the importance of central (low l-wave) collisions, which emphasize the attractive nuclear interaction, is enhanced. In addition, low relative energy allows the changing internuclear potential to effectively couple with collective excitations in the two nuclei, resulting in a fusion enhancement. These expectations are supported by the observation of an enhancement at sub-barrier energies for the mass asymmetric system $^{15}C + ^{232}Th$ [9].

* Corresponding author.
*E-mail address:* deSouza@indiana.edu (R.T. deSouza).

http://dx.doi.org/10.1016/j.physletb.2016.12.017
0370-2693/

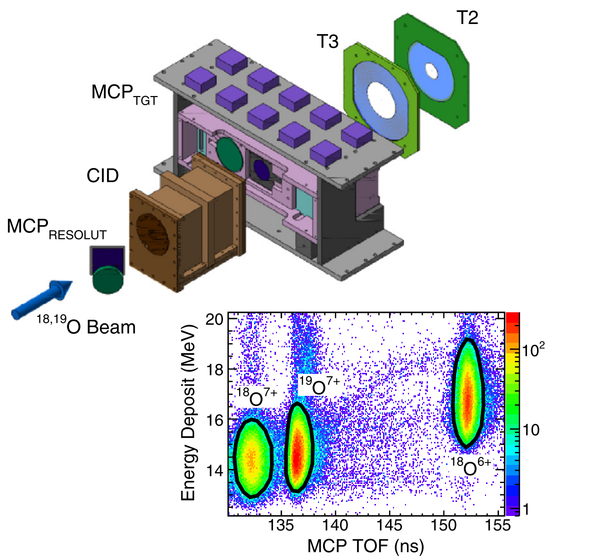


**Fig. 1.** (Color online) Schematic illustration of the experimental setup. The MCP$_{RESOLUT}$ detector is located approximately 3.5 m upstream of the compact ionization chamber (CID) which is situated directly in front of the MCP$_{TGT}$ detector. Evaporation residues are detected in the annular silicon detectors designated T2 and T3. Inset: Energy deposit versus time-of-flight spectrum for ions exiting RESOLUT that are incident on $^{12}$C target at E$_{lab}$ = 46.7 MeV. Color is used to represent yield in the two-dimensional spectrum.

To definitively establish if neutron-rich light nuclei in more mass symmetric systems exhibit a fusion enhancement at sub-barrier energies, high quality experimental data is needed. As beams of neutron-rich nuclei far from $\beta$-stability, which will provide the most stringent test of fusion models, will be available at low intensity, it is crucial to develop an experimental technique capable of measuring the fusion cross-section using such low-intensity radioactive beams. In this work, we present for the first time a measurement of the total fusion cross-section for $^{19}$O + $^{12}$C at incident energies near the barrier and compare the results with the fusion cross-section for $^{18}$O + $^{12}$C. The experimentally measured cross-sections are then compared with a microscopic model of fusion.

The experiment was performed at the John D. Fox accelerator laboratory at Florida State University. A beam of $^{18}$O ions, accelerated to an energy of 80.7 MeV, impinged on a deuterium gas cell at a pressure of 350 torr and cooled to a temperature of 77 K. Ions of $^{19}$O were produced via a (d, p) reaction and separated from the incident beam by the electromagnetic spectrometer RESOLUT [10]. Although this spectrometer rejected most of the unreacted beam that exited the production gas cell, the beam exiting the spectrometer consisted of both $^{19}$O and $^{18}$O ions necessitating identification of each ion on a particle-by-particle basis. Identification of each incident beam particle in the beam mixture allowed the simultaneous measurement of $^{18}$O + $^{12}$C and $^{19}$O + $^{12}$C. This dual measurement provided a robust measure of the potential fusion enhancement. Not only did it provide direct comparison of the $^{19}$O and $^{18}$O induced reactions, eliminating systematic uncertainties, but it allowed the comparison of the $^{18}$O data with a prior high resolution measurement of the same reaction.

The setup used to measure fusion of oxygen ions with carbon nuclei in this experiment is depicted in Fig. 1. After exiting the RESOLUT spectrometer, particles traverse a thin foil (0.5 μm thick aluminized mylar) ejecting electrons in the process. These electrons are accelerated and bent out of the beam path and onto the surface of a microchannel plate detector (MCP$_{RESOLUT}$) where they are amplified to produce a fast timing signal. After traversing the thin foil of MCP$_{RESOLUT}$, the oxygen ions passed through a compact ionization detector (CID) located approximately 3.5 m downstream of MCP$_{RESOLUT}$. In passing through this ionization chamber, ions deposit an energy ($\Delta$E) characterized by their atomic number (Z), mass number (A), and incident energy. After exiting CID the ions are incident on a 105 μg/cm$^2$ carbon foil. This carbon foil serves both as a secondary electron emission foil for the target microchannel plate detector (MCP$_{TGT}$) and as the target for the fusion experiment [11]. To maximize the production cross-section for $^{19}$O it was necessary to operate at a high incident energy and not modify the pressure of the deuterium gas cell. Therefore, in order to adjust the energy of the beam incident on the target the pressure in CID was adjusted. As the gas pressure in CID can be well controlled it provides a much more uniform degrader than a solid foil. Periodic insertion of a surface barrier silicon detector directly into the beam path just prior to the target provided a measurement of the energy distribution of $^{19}$O and $^{18}$O ions incident on the target. The width, $\sigma$, of the energy distribution for $^{19}$O ions was between 400–500 keV and was principally determined by straggling in the deuterium gas cell, not CID. All the excitation functions have been corrected for the width of the energy distribution.

By utilizing the timing signals from both microchannel plate detectors together with the energy deposit in the ionization chamber, a $\Delta$E–TOF measurement is performed. This measurement allows for the identification of ions in the beam as indicated in the inset of Fig. 1. Clearly evident in the figure are three peaks associated with $^{19}$O$^{7+}$ ions, $^{18}$O$^{7+}$ ions, and $^{18}$O$^{6+}$ ions. The cleanly identified $^{19}$O ions corresponded to approximately 31% of the beam intensity with the $^{18}$O$^{7+}$ and $^{18}$O$^{6+}$ corresponding to approximately 20% and 29% respectively. The intensity of the $^{19}$O beam incident on the target was $1.5–4 \times 10^3$ ions/s. Fusion of a $^{19}$O (or $^{18}$O) nucleus in the beam together with a $^{12}$C nucleus in the target foil results in the production of an excited $^{31}$Si (or correspondingly $^{30}$Si) nucleus. For collisions near the Coulomb barrier the excitation of the fusion product is relatively modest, $E^* \approx 35$ MeV. This fusion product de-excites by evaporation of a few neutrons, protons, and $\alpha$ particles resulting in an evaporation residue (ER). Statistical model calculations [12] indicate that for a $^{31}$Si compound nucleus, the nuclei $^{30}$Si, $^{29}$Si, $^{28}$Si, $^{29}$Al, $^{28}$Al, $^{27}$Mg, and $^{26}$Mg account for the bulk of the ERs. Emission of the light particles deflects the ER from the beam direction allowing its detection and identification using two annular silicon detectors designated T2 and T3 that subtend the angular range $3.5° < \theta_{lab} < 25°$. Evaporation residues are distinguished from scattered beam, as well as emitted light particles, by measuring their time-of-flight between the MCP$_{TGT}$ detector and the silicon detectors [13] together with the energy deposit in the Si detector. Using the measured energy deposit and the time-of-flight, the mass of the ion is calculated allowing ERs to be cleanly distinguished from the incident beam [11,14].

The fusion cross-section is extracted from the measured yield of evaporation residues through the relation $\sigma_{fusion} = N_{ER}/(\epsilon_{ER} \times t \times N_I)$ where $N_I$ is the number of beam particles of a given type incident on the target, t is the target thickness, $\epsilon_{ER}$ is the detection efficiency, and $N_{ER}$ is the number of evaporation residues detected. The number $N_I$ is determined by counting the particles with the appropriate time-of-flight between the two microchannel plates that additionally have the correct identification in the $\Delta$E–TOF map depicted in the inset of Fig. 1. The target thickness, t, of 105 μg/cm$^2$ is provided by the manufacturer and has an uncertainty of ±0.5 μg/cm$^2$. The number of detected residues, $N_{ER}$, is determined by summing the number of detected residues clearly identified by the ETOF technique [14]. To obtain the detection efficiency, $\epsilon_{ER}$, a statistical model is used to describe the de-excitation of the fusion product together with the geometric acceptance of the experimental setup. The detection efficiency varied from 37%

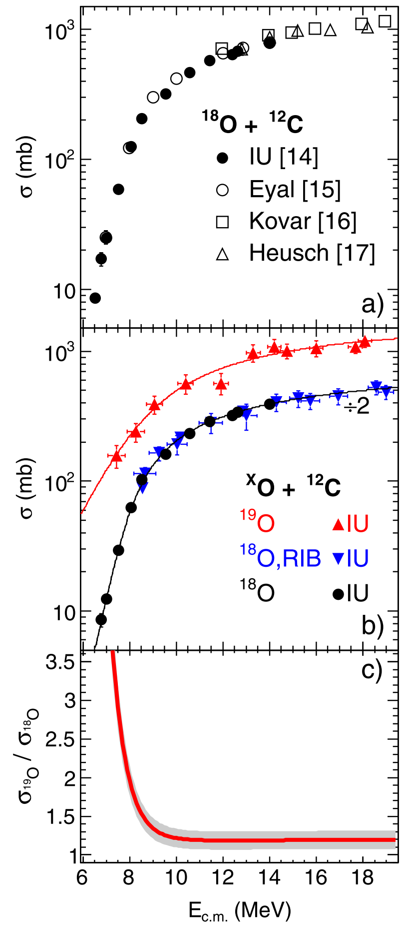


**Fig. 2.** (Color online) Fusion excitation function for $^{18,19}$O ions incident on $^{12}$C target nuclei. Panel a: Comparison of a high resolution measurement of the fusion excitation function for $^{18}O + ^{12}C$ using this experimental technique with previous measurements. Panel b: Comparison of the fusion excitation functions for $^{18,19}O + ^{12}C$ measured simultaneously in this work. For clarity, the cross-sections for the $^{18}$O induced reaction have been scaled down by a factor of two. Lines correspond to fits of experimental data as described in the text. Bottom panel: The relative cross-section, $\sigma(^{19}O)/\sigma(^{18}O)$ and is depicted as a solid line. The shaded region represents the uncertainties in the cross-section ratio. See text for details.

at the highest incident energies measured to 42% at the lowest incident energy due to the changing kinematics of the reaction.

Shown in Fig. 2a is a comparison of a high resolution measurement of the fusion excitation function for $^{18}O + ^{12}C$ (closed circles) with prior measurements reported in the literature [14–17]. This high resolution measurement was executed with a direct high quality beam of $^{18}$O and utilized a similar experimental setup to the present experiment [11,14]. Excellent agreement is observed over the entire energy interval measured down to the ≈20 mb level where the lowest energy cross-section measurement by Eyal [15] overlaps the high resolution data. This agreement indicates the validity of the present experimental technique. Presented in Fig. 2b is the dependence of the fusion cross-section on incident energy for $^{19}O + ^{12}C$ (up triangles) and $^{18}O + ^{12}C$ (down triangles) measured in the present experiment. Also shown for comparison is the high resolution measurement (closed circles) [14] for $^{18}O + ^{12}C$ presented in Fig. 2a. It is clear from Fig. 2b that the measured cross-section for the $^{18}$O beam in the present experiment (down triangles) is in good agreement with the previous high resolution measurements (closed circles), providing confidence in the radioactive beam cross-sections simultaneously measured in the present experiment.

**Table 1**
Fit parameters for the indicated fusion excitation functions. See text for details.

| | $V_C$ (MeV) | $R_C$ (fm) | $\hbar\omega$ (MeV) |
|---|---|---|---|
| $^{18}O + ^{12}C$ | 7.66 ± 0.10 | 7.39 ± 0.11 | 2.90 ± 0.18 |
| $^{19}O + ^{12}C$ | 7.73 ± 0.72 | 8.10 ± 0.47 | 6.38 ± 1.00 |

All of the excitation functions depicted in Fig. 2b manifest the same general trend. With decreasing incident energy the cross-section decreases as expected for a barrier controlled process. For clarity the cross-sections for the $^{18}$O induced reaction have been scaled down by a factor of two. At essentially all energies measured the $^{19}$O data exhibits a larger fusion cross-section as compared to the $^{18}$O data. The most important feature of the measured excitation functions is that at the lowest energies measured the fusion cross-section for the $^{19}$O system decreases more gradually with decreasing energy than does the $^{18}$O system. To examine these differences in the fusion excitation functions in more detail and quantify them we have fit the measured cross-sections with the following functional form:

$$\sigma = \frac{R_C^2}{2E}\hbar\omega \cdot ln\left\{1 + exp\left[\frac{2\pi}{\hbar\omega}(E - V_C)\right]\right\} \quad (1)$$

where $E$ is the incident energy, $V_C$ is the barrier height, $R_C$ is the radius of interaction, and $\hbar\omega$ is the barrier curvature. This functional form describes the penetration of an inverted parabolic barrier [18]. The fit of the high resolution $^{18}$O data is indicated as the solid black line in Fig. 2b. The solid red curve in Fig. 2b depicts the fit of the $^{19}$O data. With the exception of the cross-section measured at $E_{c.m.} \approx 12$ MeV, the measured $^{19}$O cross-sections are reasonably described by this parametrization. The extracted parameters for the $^{18}$O and $^{19}$O reactions are summarized in Table 1. It is not surprising that the barrier height, $V_C$, remains essentially the same for both of the reactions examined as the charge density distribution is essentially unchanged. With increasing neutron number an increase in $R_C$ is observed as one might expect. This increase in the radius can be viewed by calculating the quantity $R_C/A^{1/3}$ where A is the mass number of the compound nucleus. While for the $^{18}$O induced reaction this quantity has the value of 2.38, for the fusion of $^{19}$O, a value of 2.58 is observed. The most significant change in the fit parameters is a substantial increase in the magnitude of $\hbar\omega$ for the $^{19}$O case reflecting a narrower barrier, indicating an increased attractive nuclear potential.

Depicted in Fig. 2c as the solid (red) line is the dependence of the measured ratio of $\sigma(^{19}O)/\sigma(^{18}O)$ on $E_{c.m.}$. At energies well above the barrier $\sigma(^{19}O)/\sigma(^{18}O)$ is essentially flat at a value of ≈ 1.2. As one approaches the barrier it rapidly increases to a value of approximately 3.5. Hence, the addition of a single additional neutron in $^{19}$O as compared to $^{18}$O results in a dramatic enhancement in the fusion cross-section at sub-barrier energies.

To assess the sensitivity of our result to the low energy points, we have analyzed the data in the following manner. Re-fitting the data with elimination of the lowest energy data point results in effectively the same enhancement curve depicted in Fig. 2c. A similar result is obtained if instead, the second lowest energy data point is eliminated and the data is re-analyzed. The resulting enhancements lie well within the shaded region presented in Fig. 2c. Elimination of the two lowest energy data points (an extreme case) acts to increase the extracted enhancement. This latter result is understandable as there is no constraining data in the sub-barrier regime. These results indicate that the measured enhancement factor is robust and does not simply depend on the last data point.

In order to understand this fusion enhancement we have compared the experimental results with the predictions of a microscopic model. In recent years it has become possible to perform

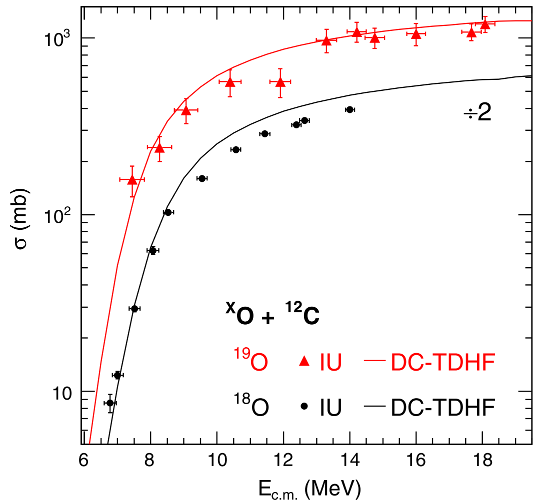


**Fig. 3.** (Color online) Comparison of the measured fusion excitation functions for $^{18,19}O$ ions incident on $^{12}C$ target nuclei with the predictions of the DC-TDHF model.

time-dependent Hartree–Fock (TDHF) calculations on a 3D Cartesian grid thus not requiring any artificial symmetry restrictions and with much more accurate numerical methods [19,20]. Over the past several years, the density constrained TDHF (DC-TDHF) method for calculating heavy-ion potentials [21] has been employed to calculate heavy-ion fusion cross-sections with considerable success [22]. While most applications have been for systems involving heavy nuclei, recently the theory was used to study above and below barrier fusion cross-sections for lighter systems, specifically for reactions involving various isotopes of O + O and O + C [23,24,14] relevant for the reactions that occur in the neutron star crust. One general characteristic of TDHF and DC-TDHF calculations for light systems is that the fusion cross-section at energies well above the barrier are usually overestimated [25,26], whereas an excellent agreement is found for sub-barrier cross-sections [23]. This overestimation is believed to be due to various breakup channels in higher energy reactions of these lighter systems that are not properly accounted for in TDHF dynamics and contribute to fusion instead. Nevertheless, the agreement is remarkable given the fact that the only input in DC-TDHF is the Skyrme effective nucleon–nucleon interaction, and there are no adjustable parameters. The DC-TDHF calculations involving the $^{18}O$ nucleus requires the use of pairing to obtain a correct spherical initial Hartree–Fock state. We have used the density dependent pairing with the SV-bas Skyrme parametrization [27] to achieve this. This nucleus with frozen occupations was then used in the TDHF time evolution. The initial state for the $^{19}O$ nucleus requires, in addition to pairing, the use of all the time-odd interaction terms in the Skyrme interaction due to the odd neutron number, which are present in the TDHF program. In our previous paper [14] we have also performed coupled-channel calculations (CCFULL) for the $^{18}O + {}^{12}C$ system with similar results to the DC-TDHF calculations. The complex level scheme for an odd-mass nucleus necessitates information for all of the experimental transitions. Inclusion of only some levels requires inclusion of an imaginary potential to account for the neglected ones complicating the calculation for $^{19}O$ significantly.

Presented in Fig. 3 is a comparison of the measured fusion cross-sections with those predicted by the DC-TDHF model. While the model provides a reasonable description of the fusion excitation function for $^{19}O$ in the energy regime measured, its description of the fusion excitation function for $^{18}O$ is notably poorer. Closer examination of the $^{18}O$ excitation function reveals that the model overpredicts the cross-section at above barrier energies but provides a good description in the interval 7.5 MeV < $E_{c.m.}$ < 8.5 MeV. For even lower energies than those depicted here it has been demonstrated that the DC-TDHF calculations underpredict the experimental cross-sections [14]. As the treatment of pairing within the initial nuclei is known to have a significant influence on the fusion excitation function [14], it is reasonable to hypothesize that the better prediction for $^{19}O$ is due to the lack of pairing in the last valence neutron of $^{19}O$. By extending the measurement of the $^{19}O$ excitation function to lower energies as well as performing a high quality measurement of $^{20,21}O + {}^{12}C$ this hypothesis could be tested. The availability of these neutron-rich oxygen beams at the GANIL/SPIRAL1 facility in Caen, France makes this measurement feasible.

In summary, we have developed an experimental technique to directly measure fusion induced by low-intensity radioactive beams ($10^3$–$10^6$ ions/s). Using this approach we have measured for the first time the fusion of $^{19}O + {}^{12}C$ at incident energies near and below the barrier to investigate whether fusion of neutron-rich light nuclei is enhanced relative to their $\beta$ stable isotopes. Comparison of the fusion excitation function for $^{19}O + {}^{12}C$ with that of $^{18}O + {}^{12}C$, clearly demonstrates that for the $^{19}O$ system, fusion is significantly enhanced. Well above the barrier this enhancement is approximately 20% which can be related to an increase in the radius due to the presence of the additional neutron. Near and below the barrier the fusion enhancement is even more dramatic, increasing to more than a factor of three at the lowest energy measured. Comparison of the experimental data with a microscopic model revealed that the DC-TDHF model was capable of describing fusion in the $^{19}O + {}^{12}C$ system. The improved description of the $^{19}O$ reaction as compared to $^{18}O$ may signal the diminished importance of pairing in the $^{19}O$ fusion reaction. This result motivates measurement of fusion, using this technique, for even more neutron-rich oxygen nuclei at energies near and below the barrier to elucidate the defining characteristics of this fusion enhancement.[1]

## Acknowledgements

We wish to acknowledge the support of the staff at Florida State University's John D. Fox accelerator in providing the high quality beam that made this experiment possible. This work was supported by the U.S. Department of Energy under Grant Nos. DE-FG02-88ER-40404 (Indiana University), DE-FG02-87ER40365 (Indiana University Nuclear Theory), DE-SC0008808 (NUCLEI SciDAC Collaboration), DE-FG02-02ER-41220 (Florida State University), DE-SC0013847 (Vanderbilt University) and the National Science Foundation under Grant No. PHY-1491574 (Florida State University). J.V. acknowledges the support of a NSF Graduate Research Fellowship under Grant No. 1342962.

## References

[1] J.F. Liang, D. Shapira, C.J. Gross, J.R. Beene, J.D. Bierman, A. Galindo-Uribarri, J. Gomez del Campo, P.A. Hausladen, Y. Larochelle, W. Loveland, P.E. Mueller, D. Peterson, D.C. Radford, D.W. Stracener, R.L. Varner, Phys. Rev. Lett. 91 (2003) 152701.

[2] W. Loveland, A.M. Vinodkumar, R.S. Naik, P.H. Sprunger, B. Matteson, J. Neeway, M. Trinczek, M. Dombsky, P. Machule, D. Ottewell, D. Cross, K. Gagnon, W.J. Mills, Phys. Rev. C 74 (2006) 064609.

[3] A. Lemasson, A. Shrivastava, A. Navin, M. Rejmund, N. Keeley, V. Zelevinsky, S. Bhattacharyya, A. Chatterjee, G. de France, B. Jacquot, V. Nanal, R.G. Pillay, R. Raabe, C. Schmitt, Phys. Rev. Lett. 103 (2009) 232701.

[1] Experiments to investigate near-barrier fusion in $^{20,21}O + {}^{12}C$ and $^{39,47}K + {}^{28}Si$ at GANIL and at MSU-NSCL respectively are presently underway.

[4] J.J. Kolata, A. Roberts, A.M. Howard, D. Shapira, J.F. Liang, C.J. Gross, R.L. Varner, Z. Kohley, A.N. Villano, H. Amro, W. Loveland, E. Chavez, Phys. Rev. C 85 (2012) 054603.
[5] Z. Kohley, J.F. Liang, D. Shapira, C.J. Gross, R.L. Varner, J.M. Allmond, J.J. Kolata, P.E. Mueller, A. Roberts, Phys. Rev. C 87 (2013) 064612.
[6] C.J. Horowitz, E.F. Brown, Y. Kim, W.G. Lynch, R. Michaels, A. Ono, J. Piekarewicz, M.B. Tsang, H.H. Wolter, J. Phys. G 41 (2014) 093001.
[7] M.J. Rudolph, Z.Q. Gosser, K. Brown, S. Hudan, R.T. deSouza, A. Chbihi, B. Jacquot, M. Famiano, J.F. Liang, D. Shapira, D. Mercier, Phys. Rev. C 85 (2012) 024605.
[8] P.F.F. Carnelli, S. Almaraz-Calderon, K.E. Rehm, M. Albers, M. Alcorta, P.F. Bertone, B. Digiovine, H. Esbensen, J.O. Fernández Niello, D. Henderson, C.L. Jiang, J. Lai, S.T. Marley, O. Nusair, T. Palchan-Hazan, R.C. Pardo, M. Paul, C. Ugalde, Phys. Rev. Lett. 112 (2014) 192701.
[9] M. Alcorta, K.E. Rehm, B.B. Back, S. Bedoor, P.F. Bertone, C.M. Deibel, B. DiGiovine, H. Esbensen, J.P. Greene, C.R. Hoffman, C.L. Jiang, J.C. Lighthall, S.T. Marley, R.C. Pardo, M. Paul, A.M. Rogers, C. Ugalde, A.H. Wuosmaa, Phys. Rev. Lett. 106 (2011) 172701.
[10] I. Wiedenhöver, L.T. Baby, D. Santiago-Gonzalez, A. Rojas, J.C. Blackmon, G.V. Rogachev, J. Belarge, E. Koshchiy, A.N. Kuchera, L.E. Linhardt, J. Lail, K.T. Macon, M. Matos, B.C. Rascol, Studies of exotic nuclei at the RESOLUT facility of Florida State University, in: J.H. Hamilton, A.V. Ramayya (Eds.), Fifth International Conference on Fission and Properties of Neutron-Rich Nuclei, World Scientific, 2013, pp. 144–151.
[11] T.K. Steinbach, M.J. Rudolph, Z.Q. Gosser, K. Brown, B. Floyd, S. Hudan, R.T. deSouza, J.F. Liang, D. Shapira, M. Famiano, Nucl. Instrum. Methods Phys. Res., Sect. A 743 (2014) 5.
[12] N.G. Nicolis, J.R. Beene, 1993, unpublished.
[13] R.T. deSouza, A. Alexander, K. Brown, B. Floyd, Z.Q. Gosser, S. Hudan, J. Poehlman, M.J. Rudolph, Nucl. Instrum. Methods Phys. Res., Sect. A 632 (2011) 133.
[14] T.K. Steinbach, J. Vadas, J. Schmidt, C. Haycraft, S. Hudan, R.T. deSouza, L.T. Baby, S.A. Kuvin, I. Wiedenhöver, A.S. Umar, V.E. Oberacker, Phys. Rev. C 90 (2014) 041603(R).
[15] Y. Eyal, M. Beckerman, R. Checkhik, Z. Fraenkel, H. Stocker, Phys. Rev. C 13 (1976) 1527.
[16] D.G. Kovar, D.F. Geesaman, T.H. Braid, Y. Eisen, W. Henning, T.R. Ophel, M. Paul, K.E. Rehm, S.J. Sanders, P. Sperr, J.P. Schiffer, S.L. Tabor, S. Vigdor, B. Zeidman, F.W. Prosser Jr., Phys. Rev. C 20 (1979) 1305.
[17] B. Heusch, C. Beck, J.P. Coffin, P. Engelstein, R.M. Freeman, G. Guillaume, F. Haas, P. Wagner, Phys. Rev. C 26 (1982) 542.
[18] C.Y. Wong, Phys. Rev. Lett. 31 (1973) 766.
[19] A.S. Umar, V.E. Oberacker, Phys. Rev. C 73 (2006) 054607.
[20] J.A. Maruhn, P.-G. Reinhard, P.D. Stevenson, A.S. Umar, Comput. Phys. Commun. 185 (2014) 2195.
[21] A.S. Umar, V.E. Oberacker, Phys. Rev. C 74 (2006) 021601(R).
[22] B.B. Back, H. Esbensen, C.L. Jiang, K.E. Rehm, Rev. Mod. Phys. 86 (2014) 317.
[23] A.S. Umar, V.E. Oberacker, C.J. Horowitz, Phys. Rev. C 85 (2012) 055801.
[24] R.T. deSouza, S. Hudan, V.E. Oberacker, A.S. Umar, Phys. Rev. C 88 (2013) 014602.
[25] C. Simenel, R. Keser, A.S. Umar, V.E. Oberacker, Phys. Rev. C 88 (2013) 024617.
[26] A.S. Umar, C. Simenel, V.E. Oberacker, Phys. Rev. C 89 (2014) 034611.
[27] P. Klüpfel, P.-G. Reinhard, T.J. Bürvenich, J.A. Maruhn, Phys. Rev. C 79 (2009) 034310.